

## Research Article

### Effect of Cutting Tool Geometry on Morphology of flank Wear Land in Turning of Low Carbon Steels

K. Khalili and M. Danesh

Department of Mechanical Engineering, The University of Birjand, Birjand, Iran

**Abstract:** The amount of flank wear is often used as the criterion for tool life assessment because it influences work material surface roughness and accuracy. In this study, the influence of cutting tool geometry (angles) on morphology of flank wear land during turning of low carbon steel is investigated by using image processing techniques and Response Surface Methodology (RSM). The analysis was based on a second order model in which the flank wear (area and shape factors) is expressed as a function of three cutting tool geometry parameters (relief angle, rake angle and cutting edge angle) and the effect of tool geometry parameters and their interactive effect on flank wear land morphology have been investigated. It is found that the area and shape factors of flank wear land are highly affected by the cutting tool geometry parameters considered in the present study.

**Keywords:** Cutting tool geometry, flank wear, image processing, shape factors

## INTRODUCTION

Tool wear has been identified as the most undesirable characteristic of machining operations. Most important of the tool wear types are flank wear and crater wear (Fig. 1). Flank wear occurs on the relief face of the tool edge and results in the formation of a wear land. Rubbing of the wear land against the machined surface damages the surface of work piece and reduce dimensional accuracy. Crater wear appears on the rake face of the tool and affects the mechanics of the process (Boothroyd and Knight, 2006). Commonly the measurements are performed manually using a toolmakers microscope. In the standard (International Organization for Standardization, 1993) manual measurement is defined as the way to measure the wear. The complex nature of the tool wear complicates the task of defining the flank and crater wear boundaries manually. Obviously, the process is time consuming and limited in accuracy and application. To overcome these problems, advances in computer vision technology have led to the investigation of its application in tool wear measurement (Jurkovic *et al.*, 2005).

The measurements defined for flank wear in the standard are shown in Fig. 2. These measures are  $V_B$  and  $V_{B\max}$ .

On the other hand, image analysis, due to its high information content is an effective tool to investigate shape of wear zone. The use of machine vision in the determination and investigation of tool wear is fairly wide spread in the manufacturing literature. Kurada and Bradley (1997) in their review paper summarized a

range of computer vision techniques applied to tool condition monitoring. Kerr *et al.* (2006) described the use of digital image processing techniques in the analysis of images of worn cutting tools in order to assess their degree of wear and remaining useful life. Wang *et al.* (2006) proposed a threshold-independent approach based on machine vision system to measure flank wear of a cutting tool. Shahabi *et al.* (2009a, b) developed a vision based method that can be used to detect notch wear from a single image of cutting tool in the micrometer range. In their other research (2009) the flank wear land width in zone C ( $V_{BC}$ ) was measured using 2-D images of nose profile and the workpiece roughness profile. Schmitt *et al.* (2012) developed a machine vision system for automated tool wear inspection. The proposed approach measures the tool wear region based on the active contour algorithm and classifies the wear type by means of neural networks.

In this study, image processing techniques and response surface methodology is used to investigate the relationship between tool edge geometry parameters (e.g., relief angle, rake angle and cutting edge angle) on the morphology characteristics of flank wear land (e.g., the area and shape factors). The results show that area and shape factors of flank wear land is highly affected by the geometry of cutting tool and some of them has linear relationship.

## METHODOLOGY

The cutting tests were carried out on a TN50D lathe. For this study, low carbon steel bars and HSS tool

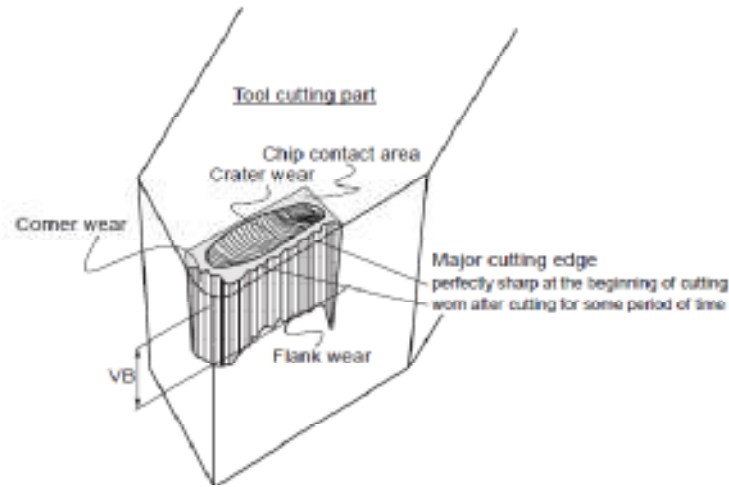


Fig. 1: Flank wear and crater wear on turning tools

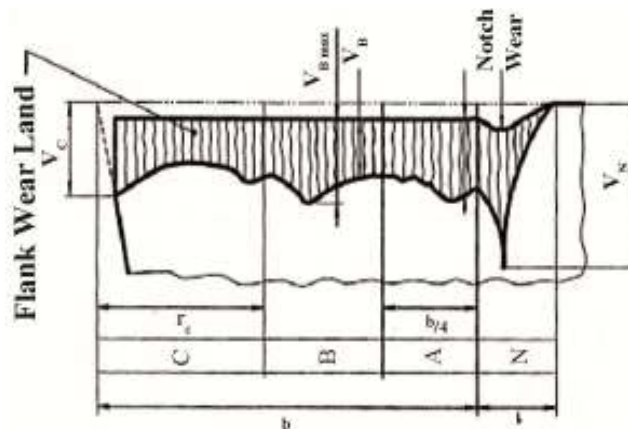


Fig. 2: Measurement of flank wears (ISO 3685)

Table 1: Levels of cutting tool geometry

Level	Relief angle ( $\alpha$ )	Rake angle ( $\gamma$ )	Cutting edge angle ( $\chi$ )
1	5	0	45
2	10	15	67.5
3	15	30	90

bits were used. The cutting speed, feed rate and depth of cut were kept constant as 47 m/min, 0.08 mm/rev and 3 mm, respectively. The tests were designed according to full factorial design and no cutting fluid was used during the turning operations. Totally, 27 experiments ( $3^3$ ) were performed by the combinations of cutting tool geometries that are given in Table 1.

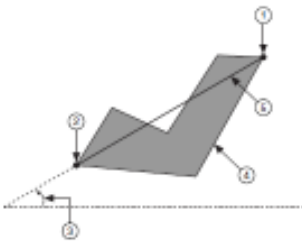
The cutting tools were prepared using a universal grinding machine. To make sure that the tool is placed at the correct and same position every time the tool has been changed, a special tool holder was designed and built. The machining for each tool was generally carried out for a fixed time.

**Image acquisition and processing:** In this study, the morphology of flank wear of the tools (including the area and shape factors) was measured by means of a machine vision system. The vision system comprises a microscope, fixture, CCD camera (3648×2736 pixels), PC and image analysis software. To eliminate the need for considering aspect ratio in camera calibration process, the sensor coordinate system was aligned with the edge of side relief surface of cutting tools as the tools are held by fixture. Table 2 lists the shape factor measurements that are used in this study.

Images of the worn tools at the end of testing are shown in Fig. 3 for some of experiments. The area and shape factors of flank wear land for different geometry's of cutting tool are shown in Table 3.

**Mathematical modeling of morphology of flank wear land:** Response Surface Methodology (RSM) is a

Table 2: Shape factors (NI vision concepts manual)

Measurement	Definition
Max feret diameter	 <ol style="list-style-type: none"> <li>1. Max feret diameter start-highest, leftmost of the two points defining the max feret diameter</li> <li>2. Max feret diameter end-lowest, rightmost of the two points defining the max feret diameter</li> <li>3. Max feret diameter orientation</li> <li>4. Particle perimeter</li> <li>5. Max feret diameter</li> </ol>
Equivalent rect short side (feret)	Shortest side of the rectangle with the same area as the particle, and longest side equal in length to the max feret diameter
Heywood circularity factor	Perimeter divided by the circumference of a circle with the same area. The closer the shape of a particle is to a disk, the closer the Heywood circularity factor is to 1
Type factor	Factor relating area to moment of inertia
Elongation factor	Max feret diameter divided by equivalent rect short side (feret). The more elongated the shape of a particle, the higher its elongation factor
Compactness factor	Area divided by the product of bounding rect width and bounding rect height. The compactness factor belongs to the interval [0, 1]

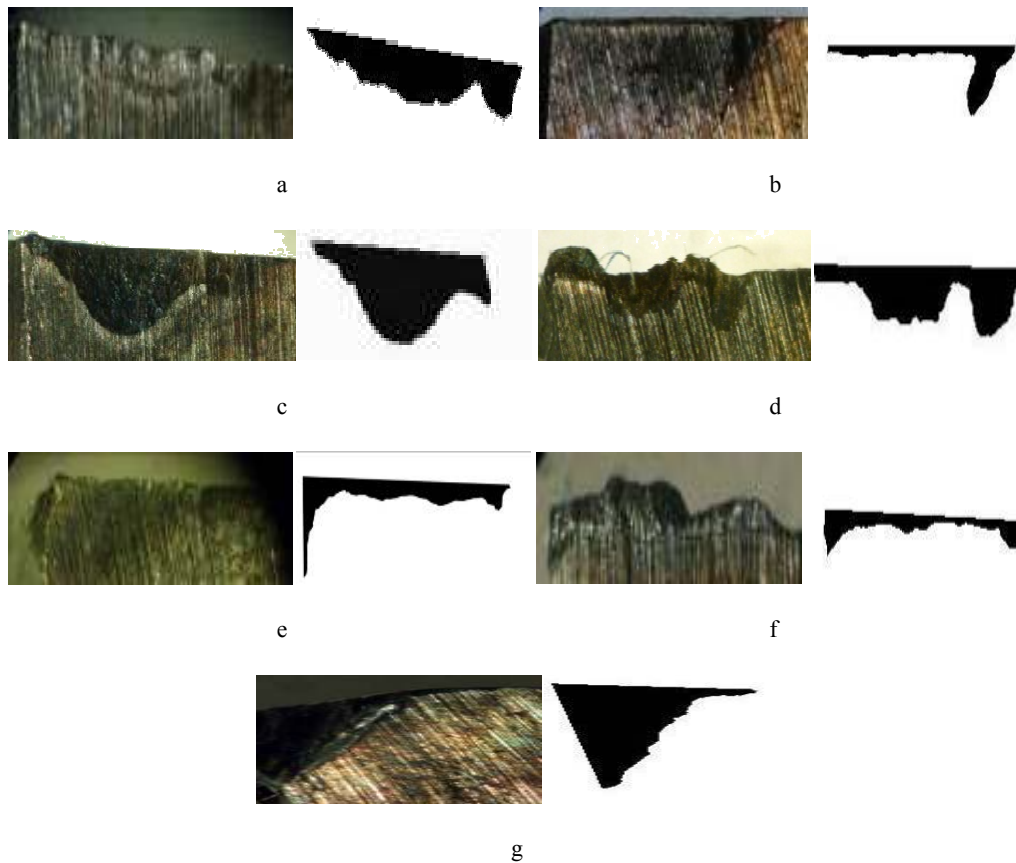


Fig. 3: Flank wear at the end of cutting (a)  $\alpha = 15$ ,  $\gamma = 0$  and  $\chi = 45$ , (b)  $\alpha = 10$ ,  $\gamma = 15$  and  $\chi = 45$ , (c)  $\alpha = 10$ ,  $\gamma = 0$  and  $\chi = 67.5$ , (d)  $\alpha = 15$ ,  $\gamma = 0$  and  $\chi = 67.5$ , (e)  $\alpha = 15$ ,  $\gamma = 15$  and  $\chi = 67.5$ , (f)  $\alpha = 5$ ,  $\gamma = 30$  and  $\chi = 67.5$ , (g)  $\alpha = 15$ ,  $\gamma = 0$  and  $\chi = 90$

Table 3: Different geometry's and results

Exp. No	$\alpha$	$\gamma$	$\chi$	Area ( $Y_{Area}$ ) (mm <sup>2</sup> )	Elongation factor ( $Y_{EF}$ )	Compactness factor ( $Y_{CF}$ )	Heywood circularity factor ( $Y_{HCF}$ )	Type factor ( $Y_{TF}$ )
1	5	0	45	0.129	12.885	0.299	3.437	0.506
2	10	0	45	0.527	8.071	0.618	1.805	0.860
3	15	0	45	0.380	9.403	0.434	2.067	0.690
4	5	15	45	0.286	4.643	0.381	2.076	0.558
5	10	15	45	0.275	7.327	0.225	2.886	0.260
6	15	15	45	0.123	33.890	0.149	4.089	0.208
7	5	30	45	0.168	23.730	0.211	3.450	0.268
8	10	30	45	0.454	17.915	0.148	2.858	0.243
9	15	30	45	0.116	34.967	0.154	4.571	0.147
10	5	0	67.5	1.031	2.596	0.575	1.435	0.836
11	10	0	67.5	0.663	4.249	0.531	1.565	0.817
12	15	0	67.5	0.445	7.588	0.459	2.262	0.717
13	5	15	67.5	0.319	8.215	0.547	2.020	0.859
14	10	15	67.5	0.145	16.765	0.540	2.688	0.714
15	15	15	67.5	0.218	8.895	0.309	2.607	0.678
16	5	30	67.5	0.140	11.916	0.553	2.310	0.810
17	10	30	67.5	0.099	27.062	0.327	3.343	0.571
18	15	30	67.5	0.228	13.115	0.303	2.654	0.409
19	5	0	90	3.024	3.382	0.587	1.362	0.884
20	10	0	90	2.862	2.876	0.587	1.302	0.869
21	15	0	90	1.426	2.748	0.410	1.514	0.724
22	5	15	90	2.349	3.879	0.514	1.439	0.840
23	10	15	90	0.373	4.267	0.182	2.954	0.245
24	15	15	90	1.942	2.700	0.566	1.309	0.870
25	5	30	90	0.208	2.993	0.104	3.510	0.106
26	10	30	90	0.109	28.877	0.345	3.956	0.419
27	15	30	90	0.136	9.378	0.328	2.980	0.453

collection of mathematical and statistical techniques that are useful for modeling and analysis of problems in which output or response is influenced by several input variables and the objective is to find the correlation between the response and the variables investigated (Montgomery, 2001). In this study second order polynomial response surface mathematical models is used for determining the relations between the cutting tool geometry parameters on the area and shape factors of flank wear land. The second-order model is normally used when the response function is not known or nonlinear. The mathematical models between morphology of wear land (area and Shape factors) and the tool geometry (relief angle ( $\alpha$ ), rake angle ( $\gamma$ ) and cutting edge angle ( $\chi$ ) of cutting tool) obtained from the response surface methodology analysis are given as follow:

The model obtained for area of flank wear land:

$$Y_{area} = -0.17325 - 0.0085124 \alpha + 0.027291 \gamma - 0.01726 \chi + (1) \\ 0.0010285 \alpha^2 + 0.000088391 \alpha\gamma - 0.00033181 \alpha\chi - \\ 0.0001059 \gamma^2 - 0.00064856 \gamma\chi + 0.00029288 \chi^2$$

The model obtained for compactness factor:

$$Y_{CF} = -4.41736 - 0.015756 \alpha - 0.0099463 \gamma + 0.030801 \chi - (2) \\ 0.00027333 \alpha^2 + 0.000083333 \alpha\gamma + 0.00018741 \alpha\chi + \\ 0.000036296 \gamma^2 + 0.0000076543 \gamma\chi - 0.00022453 \chi^2$$

The model obtained for elongation factor:

$$Y_{EF} = 4.599 + 2.3037 \alpha - 0.090673 \gamma + 0.17201 \chi - (3) \\ 0.073735 \alpha^2 + 0.0099473 \alpha\gamma - 0.009175 \alpha\chi + \\ 0.0068463 \gamma^2 + 0.0014191 \gamma\chi - 0.0022378 \chi^2$$

The model obtained for Heywood circularity factor:

$$Y_{HCF} = 3.6598 + 0.19029 \alpha - 0.026733 \gamma - 0.069597 \chi - (4) \\ 0.0048357 \alpha^2 + 0.00053712 \alpha\gamma - 0.0010584 \alpha\chi + \\ 0.00034222 \gamma^2 + 0.00086445 \gamma\chi + 0.00036224 \chi^2$$

The model obtain for type factor:

$$Y_{TF} = -0.80725 - 0.057633 \alpha - 0.0093056 \gamma + 0.055164 \chi + \\ 0.00126 \alpha^2 - 0.000088889 \alpha\gamma + 0.00037333 \alpha\chi - \\ 0.00003333 \gamma^2 - 0.000024938 \gamma\chi - 0.00040296 \chi^3 (5)$$

## RESULTS AND DISCUSSION

The analysis of the effects of the cutting tool geometry variables (relief angle ( $\alpha$ ), rake angle ( $\gamma$ ) and cutting edge angle ( $\chi$ )) on the flank wear area were performed based on Eq. (1). Figure 4 illustrates the effect of relief angle on the flank wear area for different rake angles. It can be seen that increase in relief angle

causes a decrease in flank wear area especially at lower levels of rake angles.

The effect of rake angle on the flank wear area for different relief angles is shown in Fig. 5. It can be observed that an increase of rake angle causes a decrease in area of flank wear land. This phenomenon could be explained by the fact that the increase in rake angle decreases the formation of Built up Edge (BUE) (Fang and Dewhurst, 2005), which will result in a decrease in the flank wear.

Figure 6 shows the effect of cutting edge angle on the flank wear area for different rake angles. The figure indicates that the flank wear area increases with the increase of cutting edge angle for lower values of rake angle.

Analyzing the effects of cutting tool geometry parameters on the compactness factor has been

performed based on Eq. (2). Figure 7 shows the effect of rake angle on the compactness factor for different relief angles. It can be seen that there is a linear correlation between the compactness factor and rake angle.

Figure 8 shows the effect of relief angle on the compactness factor for different rake angles. It is clear that relief angle has a linear effect on the compactness factor.

Figure 9 shows the effect of cutting edge angle on the compactness factor for different rake angles. It is observed from the figure that with the increase in the cutting edge angle up to  $70^\circ$ , the compactness factor increases thereafter decreases.

The relation between geometry parameters and elongation factor has been studied based on Eq. (3).

Figure 10 shows the effect of rake angle and cutting edge angle on the elongation factor. It can be

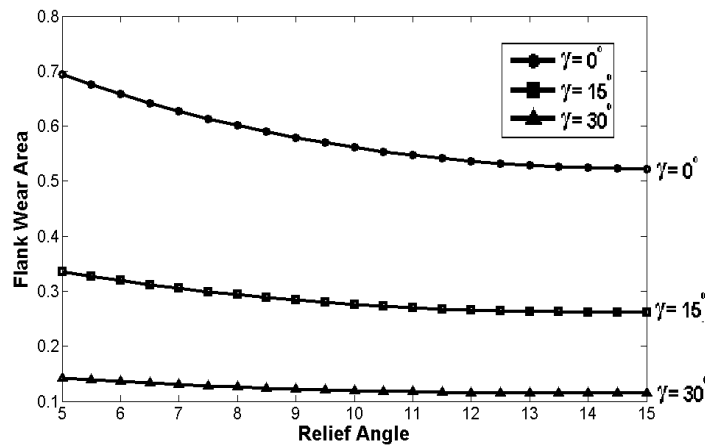


Fig. 4: Effect of relief angle on the flank wear area for different rake angles

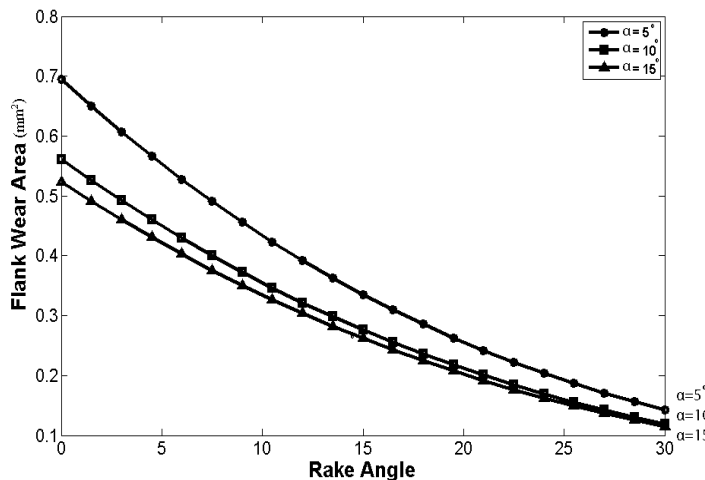


Fig. 5: Effect of rake angle on the flank wear area for different relief angles

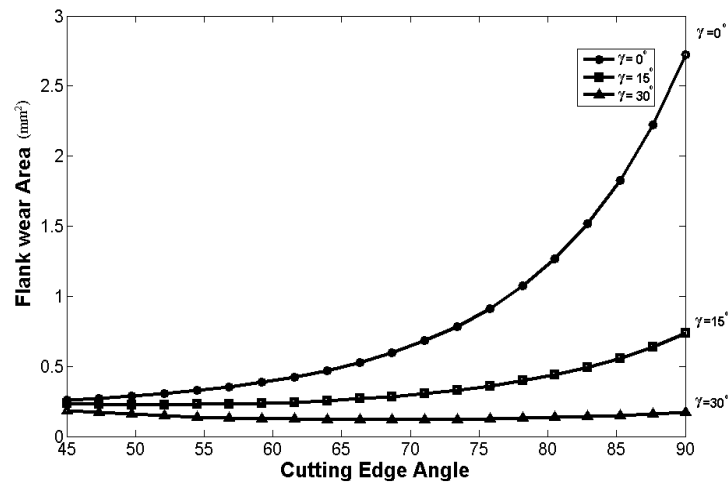


Fig. 6: Effect of cutting edge angle on the flank wear area for different rake angles

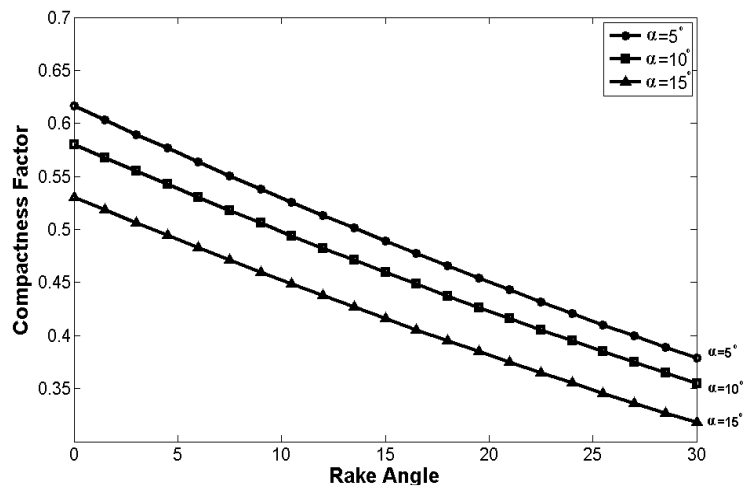


Fig. 7: Effect of rake angle on the compactness factor for different relief angles

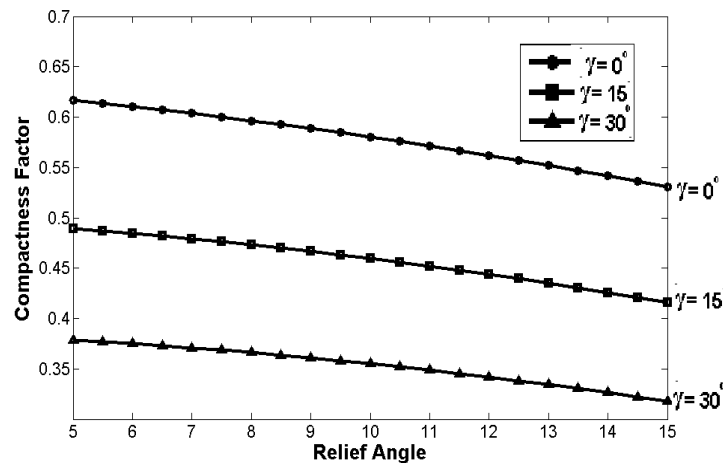


Fig. 8: Effect of relief angle on the compactness factor for different rake angles

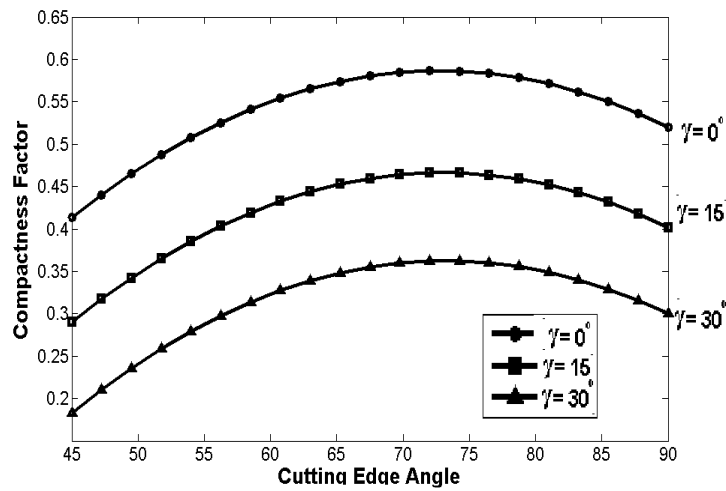


Fig. 9: Effect of cutting edge angle on the compactness factor for different rake angles

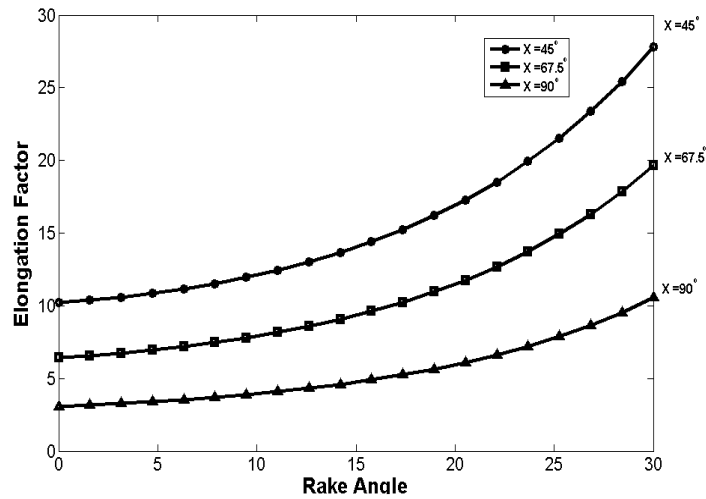


Fig. 10: Effect of rake angle cutting edge angle on the elongation factor for different cutting edge angles

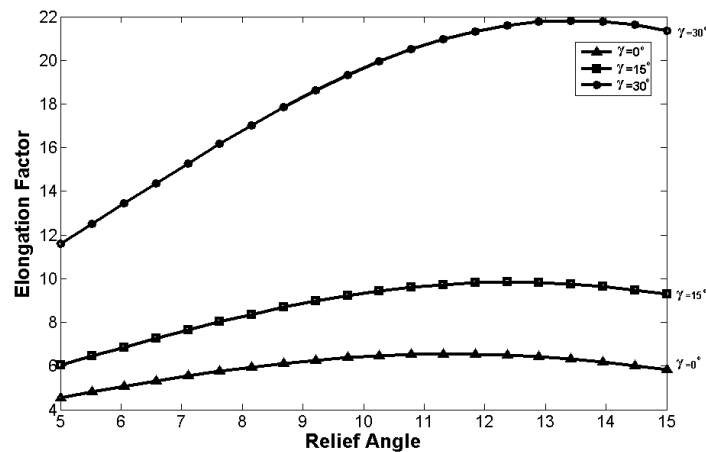


Fig. 11: Effect of relief angle on the elongation factor for different rake angles

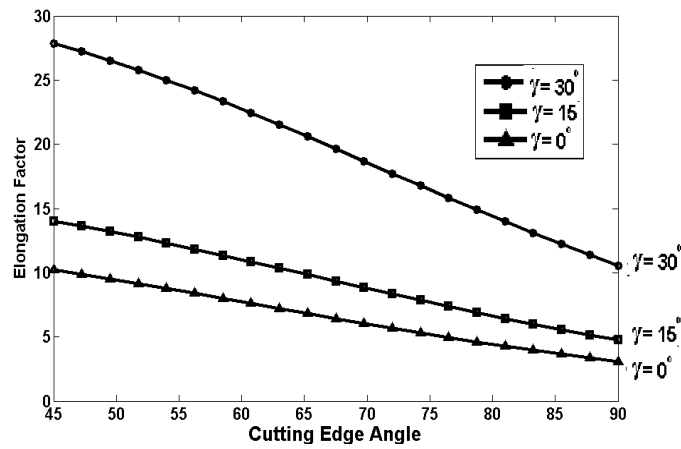


Fig. 12: Effect of cutting edge angle on the elongation factor for different rake angles

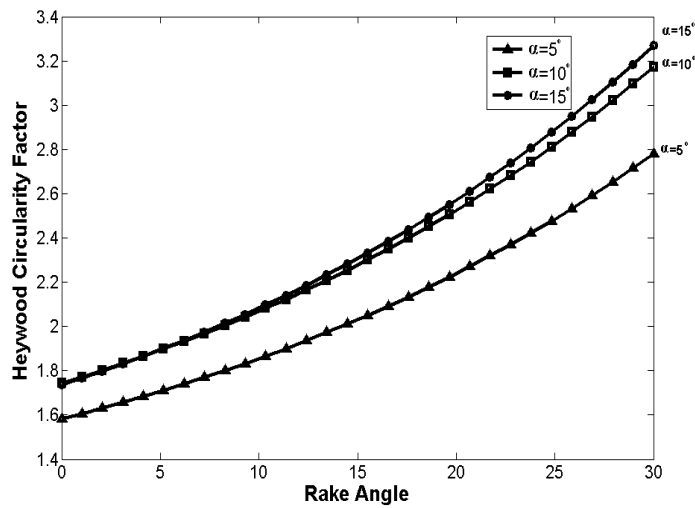


Fig. 13: Effect of rake angle and cutting edge angle on the Heywood circularity factor for different relief angles

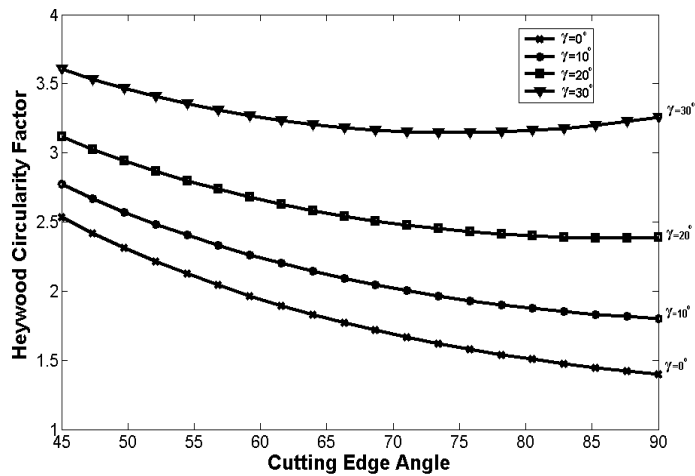


Fig. 14: Effect of cutting edge angle on the Heywood circularity factor for different rake angles



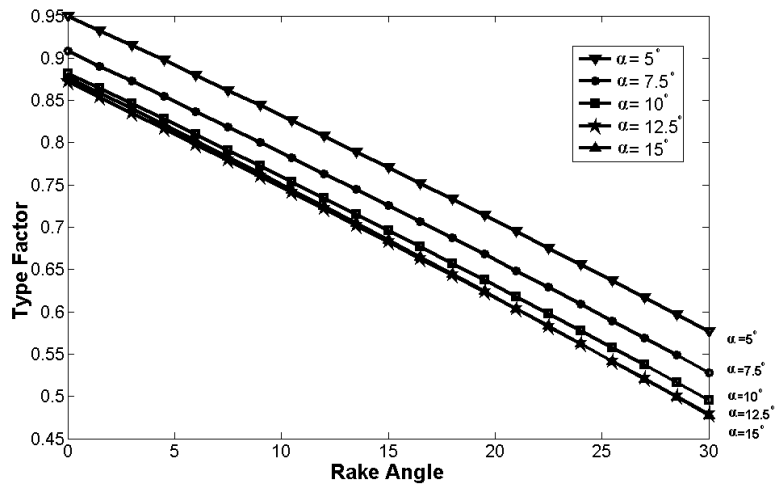


Fig. 15: Effect of rake angle on the type factor for different relief angles

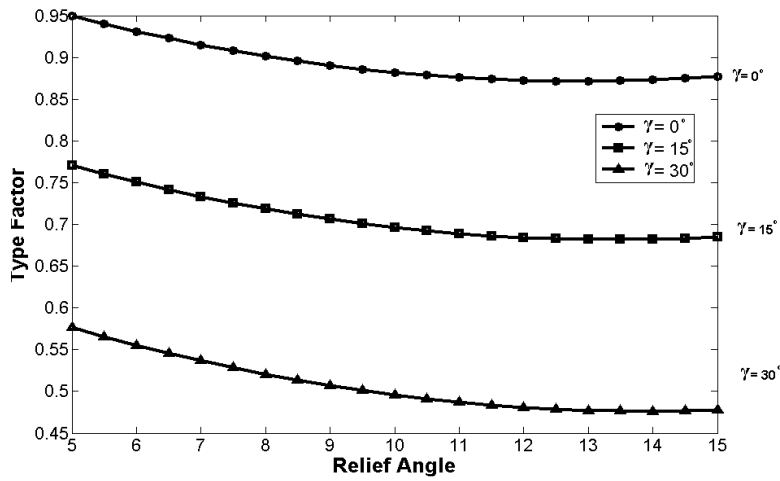


Fig. 16: Effect of relief angle on the type factor for different rake angles

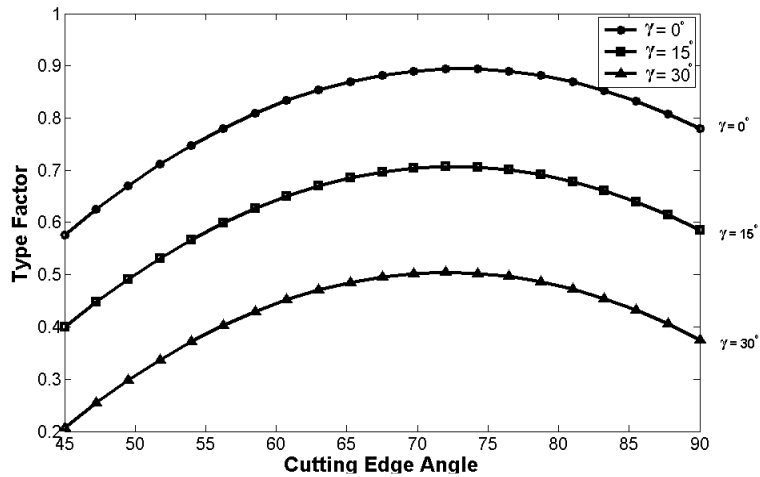


Fig. 17: Effect of cutting edge angle on the type factor for different rake angles

noticed that the elongation factor values increase with the rake angle increase for all cutting edge angles.

Figure 11 shows the effect of relief angle and rake angle on the elongation factor. It can be observed that the elongation factor increases with the increase of relief angle and at a certain relief angle the elongation factor decreases with further increase of relief angle.

The effect of cutting edge angle on the elongation factor is shown in Fig. 12. The figure indicates that elongation factor decreases with the increase of cutting edge angle.

This phenomenon could be explained by the fact that decreasing the cutting edge angle from  $90^\circ$  to  $45^\circ$  increases the length of cutting edge engagement, which will result in a longer wear land.

The relation between tool geometry on the Heywood circularity factor has been studied based on Eq. (4). Figure 13 shows effect of rake angle and cutting edge angle on the Heywood circularity factor for different relief angles. It can be seen that the Heywood circularity factor increases with an increase in the rake angle.

Figure 14 shows the effect of cutting edge angle on the Heywood circularity factor. The figure indicates that circularity of wear land decreases with the increase of cutting edge angle for lower values of rake angle.

Studying the effects of cutting tool geometry parameters on the type factor has been carried out based on Eq. (5). Figure 15 illustrates the effect of rake angle on the type factor for different relief angles. It can be seen that the type factor decreases linearly with the increase of rake angle.

The effect of relief angle on the type factor for different rake angles is shown in Fig. 16. It can be seen that the rake angle has no considerable effect on the type factor.

The effect of cutting edge angle on the type factor for different rake angles is shown in Fig. 17. It can be seen at a certain cutting edge angle the type factor decreases with further increase of cutting edge angle.

## CONCLUSION

The results of this study in analyzing the effect of cutting tool geometry on morphology of flank wear land in turning of low carbon steels with presence of BUE show that the area and shape factors of flank wear land are greatly affected by the tool geometry parameters (angles). The area of flank wear land decreases with an increase of both relief angle ( $5^\circ$ - $15^\circ$ ) and rake angle ( $0^\circ$ - $30^\circ$ ) and increases with the increase of cutting edge angle ( $45^\circ$ - $90^\circ$ ) especially for lower values of rake angle. This phenomenon could be related to the formation of BUE in lower values of both relief angle and rake angle. The compactness factor of flank wear land decreases linearly with the increase of both relief angle and rake angle and has a quadratic

correlation with cutting edge angle. The elongation factor increases with an increase of rake angle and decreases with the increase of cutting edge angle and has a quadratic correlation with relief angle. The Heywood circularity factor increases with an increase of both relief angle and rake angle and decreases with the increase of cutting edge angle for lower values of rake angle. Finally, the type factor decreases with an increase of rake angle and relatively with relief angle and has a quadratic correlation with cutting edge angle. This study helped to understanding the influence of cutting tool geometry on shape of flank wear land which may help for choosing the tool geometry.

## REFERENCES

- Boothroyd, G. and W. Knight, 2006. Fundamentals of Machining and Machine Tools. 3rd Edn., CRC Press, Taylor and Francis Group, Boca Raton.
- Fang, N. and P. Dewhurst, 2005. Slip-line modeling of built-up edge formation in machining. *Int. J. Mech. Sci.*, 47: 1079-1098.
- International Organization for Standardization, 1993. Tool-Life Testing with Single-Point Turning Tools. ISO 3685.
- Jurkovic, J., M. Korosec and J. Kopac, 2005. New approach in tool wear measuring technique using CCD vision system. *Int. J. Mach. Tools Manuf.*, 45: 1023-1030.
- Kerr, D., J. Pengilley and R. Garwood, 2006. Assessment and visualization of machine tool wear using computer vision. *Int. J. Adv. Manuf. Technol.*, 28: 781-791.
- Kurada, S. and C. Bradley, 1997. A review of machine vision sensors for tool condition monitoring. *Comput. Ind.*, 34(1): 55-72.
- Montgomery, D.C., 2001. Design and Analysis of Experiments. John Willy and Sons Inc., New York.
- Schmitt, Y., Y. Cai and A. Pavim, 2012. Machine vision system for inspecting flank wear on cutting tools. *ACEEE Int. J. Control Syst. Instrument.*, 3: 27-31.
- Shahabi, H.H., T.H. Low and M.M. Ratnam, 2009a. Notch wear detection in cutting tools using gradient approach and polynomial fitting. *Int. J. Adv. Manuf. Technol.*, 40: 1057-1066
- Shahabi, H.H., T.H. Low and M.M. Ratnam, 2009b. Assessment of flank wear and nose radius wear from workpiece roughness profile in turning operation using machine vision. *Int. J. Adv. Manuf. Technol.*, 43: 11-21.
- Wang, W.H., G.S. Hong and Y.S. Wong, 2006. Flank wears measurement by threshold independent method with sub-pixel accuracy. *Int. J. Mach. Tools Manuf.*, 46: 199-207.